International Journal of Heat and Mass Transfer 60 (2013) 713–721

Contents lists available at SciVerse ScienceDirect

International Journal of Heat and Mass Transfer

journal homepage: www.elsevier.com/locate/ijhmt

Simulation of thermocline storage for solar thermal power plants: From dimensionless results to prototypes and real-size tanks

Rocío Bayón *, Esther Rojas

Concentrating Solar Systems Unit – Thermal Storage, CIEMAT-PSA, Av. Complutense 40, 28040 Madrid, Spain

ARTICLE INFO

Article history:
Received 15 November 2012
Received in revised form 16 January 2013
Accepted 18 January 2013
Available online 14 February 2013

Keywords:
Solar thermal power plant
Thermal storage
Sensible heat
Thermocline
Prototype
Numerical simulation

ABSTRACT

A single-phase one-dimensional model called CIEMAT1D1SF has been developed for characterizing the behaviour of thermocline tanks with an effective storage medium formed by either a liquid or a liquid and a packed-bed. Despite its simplicity, this model has been validated with experimental data and the results of tank performance are similar to those obtained by other authors using more complex simulation models. In order to obtain general results the thermal equation has been nondimensionalized and the resulting expression only depends on the parameter called dimensionless velocity, v^*. It has been observed that thermocline thickness decreases as v^* increases attaining a minimum value when $v^* \geqslant 2350$ while tank efficiency increases with v^* up to a maximum of about 87% also for $v^* \geqslant 2350$. From these results the design equation for building thermocline storage tanks with maximum theoretical efficiency has been established. Since this design equation depends on tank dimensions and thermal power, small thermocline tanks and hence prototypes are not expected to behave in the same way as large or real-size tanks. Therefore maximum efficiency guideline plots for thermocline tanks with different storage media have been presented for various temperature intervals. In these plots thermal power has proven to be the critical design parameter because the larger the power the higher the degree of freedom for choosing tank dimensions and hence storage capacity and charging/discharging time. Therefore, we strongly recommend the use of these guideline plots in the design process of thermocline prototypes.

1. Introduction

Thermal storage in Solar Thermal Power Plants (STPP's) makes it possible to overcome transients and extend the operation time in order to deliver electricity when there is no solar irradiation as well as to meet peak demand independently of weather fluctuations. Up to now the storage option for extending operation time implemented in commercial STPP's is the molten salt two-tank system [1,2], whose estimated cost is about 30–50 US$ per thermal kW h [3]. Some studies have shown that these thermal storage systems have quite a significant cost reduction potential which could be between 38% and 69% by 2020 [4]. In this way, since the cost of molten salt two-tank storage systems is dominated by the tanks (30%) and the molten salt inventory (44%), one of the concepts that nowadays is being seriously considered is the molten salt based thermocline single tank with a packed-bed of low-cost solid filler. Actually the Electric Power Research Institute (EPRI) recently conducted a study where the estimated engineering, procurement and construction (EPC) costs were compared for both two-tank and packed-bed thermocline storage cases [5]. This study concluded that the thermocline option would have a potential to reduce around 33% the cost of thermal energy storage, which could not only greatly increase the utility of STPP's but also lead to a wider adoption of this technology around the world [6]. Therefore it seems that the next step for the thermocline systems is the construction of either pilot plants or small commercial unities that can demonstrate the operation of this kind of storage out of laboratory. Additionally, standardized design and modelling procedures will be required for validating the experimental results of field tests and hence for improving the design process and speed up both production and deployment of thermocline storage systems.

The majority of models previously developed for simulating thermocline storage tanks for STPP's consider packed-bed systems and are based on Schumann's one-dimensional model [7]. This model includes two heat transfer equations because it assumes that fluid and packed-bed particles have different temperatures. However, it neglects heat conduction in the fluid, heat exchange between the packed-bed particles and also thermal losses to the environment. Pacheco et al. [8] used Schumann model for simulating a thermocline tank containing molten solar salt as fluid and quartzite rock and sand as solid filler. Some years later Kolb et al. [9] improved Pacheco's model allowing thermal conduction

* Corresponding author. Tel.: +34 91 3466048; fax: +34 91 3466037.
E-mail addresses: rocio.bayon@ciemat.es (R. Bayón), esther.rojas@ciemat.es (E. Rojas).

0017-9310/$ - see front matter © 2013 Elsevier Ltd. All rights reserved.
http://dx.doi.org/10.1016/j.ijheatmasstransfer.2013.01.047

between control volumes and including thermal losses at top, bottom and tank walls. This model was implemented in TRNSYS® as Type 502 in the STEC library in order to simulate the whole performance of a STPP with a thermocline storage system [10]. Other authors proposed similar models and the main difference between them was either the procedure for solving the governing equations or the software applied. In this way both Bharathan et al. [11] and Yang et al. [12] used the commercial CFD software FLUENT® whereas Xu et al. [13] solved the heat transfer differential equations with a self written simulation code and Van Lew et al. [14] applied the numerical method of characteristics. For the particular case of liquid fluids, some of these models have shown there is little difference between fluid and solid filler temperatures since heat transfer between them is very efficient [12–14]. In such case the same temperature can be assumed for both liquid and filler particles and hence a single-phase model can be formulated for which only one heat transfer equation has to be solved. In a previous work [15], we already presented a single-phase one-dimensional model (called CIEMAT1D1SF) for simulating thermocline storage tanks with an effective storage medium formed by either a liquid or both a liquid and a packed-bed of solid filler.

In this work we have neglected thermal losses and the heat transfer equation has been expressed in dimensionless coordinates for simplifying the solving process and obtaining general results in terms of performance parameters. This new model has been successfully validated with various experimental data found in the literature for different kinds of thermocline storage tanks [8,16,17].

Simulations with CIEMAT1D1SF model have demonstrated that the performance of a thermocline tank strongly depends on design parameters like tank height and liquid velocity. Therefore small prototype tanks are not expected to behave in the same way as scaled-up thermocline tank, which means that a similarity analysis cannot be directly applied. In this way this paper presents the guidelines for building thermocline prototype tanks whose performance is representative of real size tanks.

2. Model description

2.1. Development of CIEMAT1D1SF model

The model CIEMAT1D1SF considers a single effective storage medium inside a thermocline tank (liquid or liquid plus solid filler) at a certain temperature, T, which varies with time, t, (unsteady), along the tank height, z (one-dimensional). This model also takes into account thermal losses to the environment and considers average values of thermophysical properties that are independent on temperature. The energy balance equation describing this storage system is:

$$(\rho C_p)_{eff}\frac{\partial T}{\partial t}+\varepsilon(\rho C_p)_{liquid}v_{liquid}\frac{\partial T}{\partial z}=k_{eff}\frac{\partial^2 T}{\partial z^2}-U_w a_w(T-T_\infty) \quad (1)$$

ρ	density (kg/m^3)
C_p	heat capacity (J/kg K)
ρC_p	volumetric heat capacity (J/m^3 K)
k	thermal conductivity (W/m K)
v_{liquid}	velocity of the liquid (m/s)
U_w	coefficient of thermal losses to the environment (W/m^2 K)
a_w	ratio between thermal losses area and tank volume (1/m) [$a_w = 4/D$]
D	tank diameter (m)
T_∞	ambient temperature (°C or K)
ε	porosity of the storage medium (dimensionless)
eff	sub index that refers to the effective storage medium
liquid	sub index that refers to the liquid

The porosity of a packed-bed, ε, is defined as the fraction of total volume that remains free for fluid circulation and its value is imposed by the kind of packing and the relative size of solid particles. From the theoretical point of view, ordered structures of identical spherical particles include rhombohedral and cubic packing, which place the range of attainable porosities between 0.259 and 0.476. Alternatively, disordered packings exhibit a smaller porosity range with most of them falling into the range 0.36–0.40 [18]. The porosity of mixed-size particle beds depends on the volume fraction of the large particles and the relative size of small and large particles. From the theoretical point of view [19], the minimal porosity value in this case could be as low as 0.16 or even 0.14. However, for a real packed-bed formed by non spherical particles the porosity must be experimentally obtained by measuring the free volume between particles for example with the help of a liquid.

In CIEMAT1D1SF model, the porosity is also used for calculating the effective volumetric heat capacity of the storage medium through the equation:

$$(\rho C_p)_{eff}=\varepsilon(\rho C_p)_{liquid}+(1-\varepsilon)(\rho C_p)_{solid} \quad (2)$$

where *solid* refers to the packed bed. For calculating the effective thermal conductivity different equations can be found in the literature [20]. In our simulations we have chosen, as a first approach, the simplest formulation, which also depends on packed-bed porosity:

$$k_{eff}=\varepsilon k_{liquid}+(1-\varepsilon)k_{solid} \quad (3)$$

When the tank contains only liquid, porosity equals 1 and hence $(\rho C_p)_{eff}=(\rho C_p)_{liquid}$ and $k_{eff}=k_{liquid}$.

During charge and discharge processes, thermal losses term can be neglected because the main contribution to temperature variation with time and position is the movement of thermocline zone and hence (Eq. (1)) becomes:

$$(\rho C_p)_{eff}\frac{\partial T}{\partial t}+\varepsilon(\rho C_p)_{liquid}v_{liquid}\frac{\partial T}{\partial z}=k_{eff}\frac{\partial^2 T}{\partial z^2} \quad (4)$$

This equation indicates that the results obtained will be independent on tank diameter, D, which means that the model is really one-dimensional and depends only on z coordinate. In order to simplify the solving process of (Eq. (4)), all variables have been expressed in dimensionless form by means of the following transformations:

$$\phi=\frac{T}{T_{\max}} \quad (5)$$

$$z^*=\frac{z}{L} \quad (6)$$

$$t^*=\frac{t\alpha_{eff}}{L^2} \quad (7)$$

$$v^*=\frac{\varepsilon(\rho C_p)_{liquid}Lv_{liquid}}{k_{eff}}=\frac{(\rho C_p)_{liquid}Lv_m}{k_{eff}}=\frac{v_{TC}L}{\alpha_{eff}} \quad (8)$$

where T_{max} is the maximum temperature of the tank (inlet temperature in charge or outlet temperature in discharge), L is the total tank height, α_{eff} is the effective thermal diffusivity, v_m is the velocity of the liquid at tank inlet/outlet and v_{TC} is the velocity at which thermocline zone moves. This velocity is constant and has been already introduced by other authors [12]. The expressions for calculating α_{eff}, v_m and v_{TC} are:

$$\alpha_{eff}=\frac{k_{eff}}{(\rho C_p)_{eff}} \quad (9)$$

$$v_m=\varepsilon v_{liquid} \quad (10)$$

$$v_{TC}=\frac{(\rho C_p)_{liquid}\varepsilon v_{liquid}}{(\rho C_p)_{eff}}=\frac{(\rho C_p)_{liquid}v_m}{(\rho C_p)_{eff}} \quad (11)$$

The resulting energy balance equation in dimensionless coordinates is:

$$\frac{\partial \phi}{\partial t^*} + v^* \frac{\partial \phi}{\partial z^*} = \frac{\partial^2 \phi}{\partial z^{*2}} \quad (12)$$

In the solving process of (Eq. (12)), the dimensionless volume tank was discretized in a certain number of non-overlapping control volumes, N_z, in which this equation was integrated. Each control volume was characterized by a spatial node, z_i^*, at a temperature, ϕ_i. To establish the pattern for the variation of dimensionless temperature between the nodes, different profiles can be applied depending on which term in the equation is being considered. In our particular case, only the terms of total flux (diffusive and convective) were taken into account and for them the power law scheme based on grid Peclet number [21] was chosen. Finally, for solving resulting system of equations a Runge–Kutta method of 4th and 5th order (Dormand-Prince) was applied and the calculations were performed using Matlab®.

2.2. Model results and characteristic parameters

The dimensionless results of CIEMAT1D1SF model are sets of curves representing temperature distribution, ϕ, along the tank height, z^*, for different time values, t^*, when simulation is performed at a certain v^*. A simulation can be launched from different starting conditions: (1) a certain temperature profile previous to charge or discharge, (2) a fully discharged tank at $T_{\min}(\phi_{\min} = \frac{T_{\min}}{T_{\max}})$ from which it is charged, or (3) a fully charged tank at T_{max} ($\phi_{max} = 1$) from which it is discharged. From the simulation curves various characteristic parameters of a thermocline tank can be obtained. Some of these parameters have been already proposed by other authors [22] and will be used in this paper for evaluating and discussing the behaviour of this kind of tanks. These parameters are described in the following section.

2.2.1. Thermocline thickness: TC_i^*

The thermocline is the vertical zone centred at certain position z_i^*, in which the temperature profile varies between ϕ_{min} and $\phi_{max} = 1$. Since ϕ profile is asymptotic to ϕ_{max} and ϕ_{min}, the limit of 0.001 for both $\phi - \phi_{min}$ and $\phi_{max} - \phi$ was established to define the thermocline thickness. When thermocline attains either tank top (in discharge) or tank bottom (in charge) and therefore the process finishes, its position is named as z_{end}^* and the corresponding thermocline thickness is TC_{end}^*.

2.2.2. Time of process: t_i^*

Moment at which the centre of thermocline is placed at a certain position z_i^*. When thermocline attains either tank top (in discharge) or tank bottom (in charge) and therefore the process finishes, thermocline is placed at z_{end}^* and the corresponding time is t_{end}^*. In this way, the following expression must be fulfilled:

$$z_{end}^* = v^* t_{end}^* \quad (13)$$

2.2.3. Ideal total energy, Q_{total}^{ideal}

Amount of energy that could be stored as sensible heat by a tank of height, L, and a temperature step: $T_{max} - T_{min}$. It is calculated by the expression:

$$Q_{total}^{ideal} = AL(\rho C_p)_{eff}(T_{\max} - T_{\min})[\mathrm{J}] \quad (14)$$

where A is the cross-sectional area of the cylindrical tank.

2.2.4. Stored/delivered energy $Q_{stored/delivered}$

Amount of energy, either delivered in discharge, $Q_{delivered}$, or accumulated in charge, Q_{stored}, by a thermocline tank at the end of the corresponding process. In all cases we assume that thermocline is never extracted from the tank. The expression for calculating this energy is:

$$Q_{stored/delivered} = (C_p)_{liquid}\dot{m}_{liquid}t_{end}(T_{\max} - T_{\min}) = A(\rho C_p)_{liquid}\varepsilon v_{liquid}t_{end}(T_{\max} - T_{\min})[\mathrm{J}] \quad (15)$$

2.2.5. Efficiency: η

Percentage ratio between the stored or delivered energy by the thermocline tank, $Q_{stored/delivered}$, and the ideal total energy, Q_{total}^{ideal}. It is calculated from (Eq. (14)–(16)), as:

$$\eta = \frac{Q_{stored/delivered}}{Q_{total}^{ideal}} \times 100 = \frac{v_{TC}t_{end}}{L} \times 100 = \frac{z_{end}}{L} \times 100 = z_{end}^* \times 100 \quad (16)$$

Therefore the efficiency of a certain process (initial charge or discharge) can be calculated directly from thermocline position in dimensionless coordinates at the end of this process.

3. Results and discussion

3.1. Validation of CIEMAT1D1SF model

In order to validate CIEMAT1D1SF model, different kinds of thermocline tanks for which experimental data can be found in the literature have been simulated. Obviously the dimensionless model can be applied for any specific case provided the dimensional variables are converted into the corresponding dimensionless ones. In Table 1 the main characteristics and design parameters of these tanks have been recorded together with the references from which the experimental data have been taken. The values of physical properties corresponding to the storage media used in the simulations are displayed in Table 5 of the Appendix section.

The behaviour of a thermocline tank with only liquid (water in this case) has been reproduced by taking into account the experimental data from Zurigat et al. [16]. The selected data together with the results predicted by CIEMAT1D1SF model are plotted in Fig. 1. Since experimental data correspond to transient temperature profiles at different vertical tank positions measured during an initial charge, the simulation was launched from a fully discharged tank with a flat temperature profile at $T_{min} = 25.9$ °C. As we can see, CIEMAT1D1SF model run with $N_z = 500$ predicts quite well the time evolution of thermocline region for positions far from to the top-inlet (in this case at $z = 0$ m), whereas temperatures recorded near this inlet differ from the values obtained with the model. According to previous studies [23], deviations of this type are due to the presence of turbulences originated at both inlet and outlet points, making thermocline thickness larger than expected from simulations. Since CIEMAT1D1SF model does not take

Table 1
Main characteristics and design parameters of thermocline tanks whose experimental data have been used in the validation of CIEMAT1D1SF model.

Design parameters	Kind of thermocline storage tank		
	Water tank Zurigat [16]	Solar one tank Faas [17]	Sandia lab prototype Pacheco [8]
Diameter (m)	0.4064	18.2	3
Height (m)	1.4465	12	6
Volume (m^3)	0.75	3122	42
Mass flow (kg/s)	0.098	30	3.7
T_{max} (°C)	50.8	295.2	395.9
T_{min} (°C)	25.9	179.2	289
Porosity, ε	1	0.22	0.22
Storage medium	Water	Rock/sand and Caloria Ht-43	Rock/sand and eu-$NaNO_3$/KNO_3

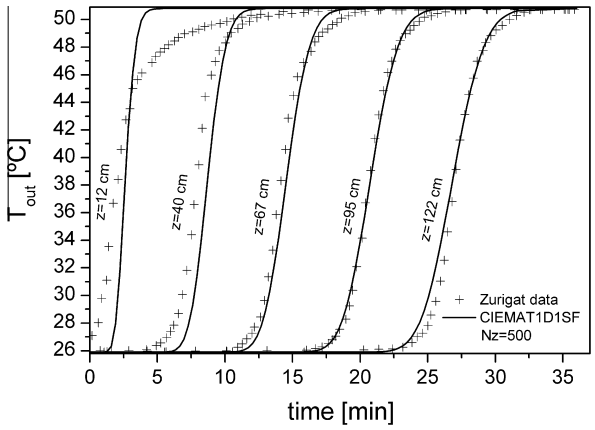

Fig. 1. Transient temperature profiles at different locations for the charging process of a water tank initially discharged at T_{min} = 25.9 °C. Comparison between the experimental data taken from Ref. [16] and the results predicted by CIEMAT1D1SF model run with N_z = 500.

into account turbulences, the mismatch in temperature profiles observed in the vicinity of top-inlet is quite reasonable.

The behaviour of thermocline tanks with both liquid and packed-bed as storage media has been reproduced by using two of the few examples for which experimental data can be found in the literature. The first example is the Solar One tank, which contained a packed-bed of sand and rock and Caloria HT-43 as storage liquid. The experimental data found correspond to a discharge process starting from a state in which thermocline is placed around the middle of tank height [17]. In Fig. 2 the spatial evolution of temperature profiles during a discharge process from 00:00 AM and 8:00 AM is displayed ('Exp-00 AM', 'Exp-04 AM' and 'Exp-08 AM' according to the figure legend). In this case, simulation was launched from the temperature profile experimentally measured at 00:00 AM and this is why the numerical profiles are not as flat as in the previous example. Again, we can see that temperature profiles predicted by CIEMAT1D1SF model ('CIEMAT1D1SF, N_z = 500' in Fig. 2) fit quite well the experimental data. These experimental results were also used by Kolb et al. [9] for validating the simulation model for thermocline tanks they developed in TRNSYS. However the slopes of their profiles ('Kolb, N_z = 23' in Fig. 2) were smaller than the slope of the experimental ones. To our opinion, the origin of this deviation is the small number of control volumes they used in their simulation, namely N_z = 23. Actually we run our model using the same number of discretized volumes and the resulting temperature profiles ('CIEMAT1D1SF, N_z = 23' in Fig. 2) were very similar to the profiles obtained by Kolb et al. [9] (see Fig. 2). Therefore, in order to obtain temperature profiles that fit the experimental measurements, we would recommend using at least 500 elementary volumes in the numerical simulations. In this way, all the simulations presented in this paper were performed under such condition.

The other example of thermocline tank with liquid and solid filler is the prototype with molten salts and packed-bed of quartzite sand and rock tested in Sandia Labs [8]. In this case experimental data also correspond to a discharge process starting from a situation in which thermocline is placed at one third of tank height. Hence the numerical simulation was launched with the temperature profile experimentally measured at 12:00 h and this is why numerical profiles are again not flat. As displayed in Fig. 3 the overall position and temperature profile of thermocline zone is predicted quite well by the model although simulated temperature points do not fit exactly the experimental values. Actually these experimental values seem to indicate important thermal losses along the top half of the tank, which may be the reason for this disagreement between some experimental points and the corresponding simulated ones.

From all the above results we can conclude that when at least 500 elementary control volumes are used, CIEMAT1D1SF model predicts reasonably well the behaviour of real thermocline tanks not only when the storage medium is a liquid fluid but also when it is combination of a liquid fluid and a packed-bed of filler materials. Since it is a one-dimensional model and considers a single phase effective storage medium, its results correspond to an ideal situation. However we have proven that it can be used for simulating thermocline tanks with a good degree of accuracy.

3.2. Dimensionless velocity, v^*, as the critical variable

Eq. (12) shows that the parameter influencing the tank behaviour and hence the one to be varied is the dimensionless velocity, v^*. This does not mean that storage medium properties (k, ρ and C_p) and packed-bed porosity (ε) have no influence on tank behaviour because actually all of them are involved in the dimensionless variables through equations (Eqs. (2), (3), (7)–(9)). However it proves the convenience of using dimensionless variables in order to obtain both general and simplified simulation results. In this way, for studying the performance of thermocline tanks,

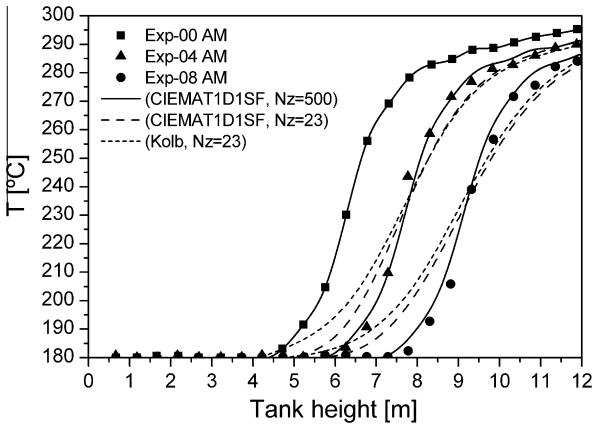

Fig. 2. Temperature profiles along tank height at different times during a discharging process of the Solar One packed-bed tank. Comparison between the experimental data taken from Ref. [17], the results predicted by CIEMAT1D1SF model (N_z = 500 and N_z = 23) and the results predicted by Kolb et al. [9] (N_z = 23).

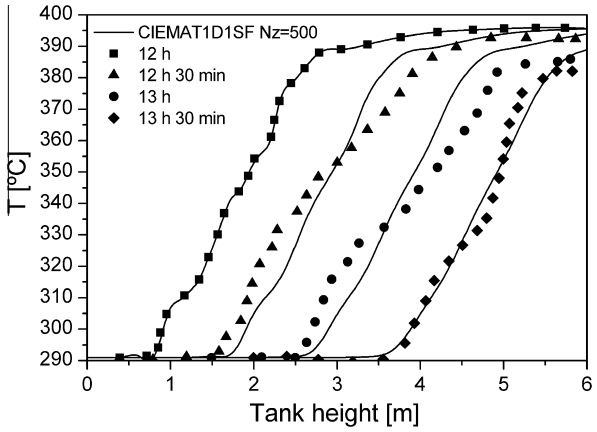

Fig. 3. Temperature profiles along tank height at different times during a discharging process of the Sandia packed-bed prototype. Comparison between the experimental data taken from Ref. [8] and the results predicted by CIEMAT1D1SF model run with N_z = 500.

simulations were carried out for dimensionless velocities, v^*, ranging from 10 to 25000. For each velocity, an initial discharge process starting from fully charged tank conditions (sub index '0') with a flat temperature profile ($\phi_0 = 1$ at $t_0^* = 0$ and $z_0^* = 0$) was simulated. Fig. 4 shows the variation of ϕ with z^* at various t_i^* for two discharge processes performed at $v_1^* = 215$ and $v_2^* = 600$. In both cases we can see that thermocline thickness increases as it moves towards the upper part of the tank (i.e. $z^* = 1$). Also we can see that thermocline thickness at the end of the process decreases as dimensionless velocity increases ($TC_{end(v2)} < TC_{end(v1)}$). Similar results were obtained by other authors that also carried out simulations of thermocline storage tanks [24]. In their case, thermocline thickness became larger as flow rate was decreased but also when time was increased. This means that in both cases thermocline has more time to develop by thermal diffusion and therefore its thickness is expected to increase.

It should be pointed out here that, if an initial charge process starting from a fully discharged tank ($\phi_0 = \phi_{min}$ at $t_0^* = 0$ and $z_0^* = 1$) were simulated, thermocline thickness at the end of the process would be the same but it would be placed at tank bottom. The values of dimensionless characteristic parameters corresponding to simulations displayed in Fig. 4 have been recorded in Table 2. In this table we can see that the greater the dimensionless velocity, v^*, the shorter the discharging time, t_{end}^*, but the higher the tank efficiency, η.

Simulations were also performed for different ϕ_{min} values and hence different temperature intervals. The resulting curves when thermocline is centred at $z^* = 0.5$ (i.e., in the middle of tank height) have been plotted in Fig. 5. As we can see, thermocline thickness is the same for all temperature intervals, which means that the characteristic parameters ($TC_{end}^*, z_{end}^*, t_{end}^*$ and η) will be independent on which temperature interval is chosen for the simulations. Xu et al. [25] also studied the influence of temperature interval in the performance of packed-bed thermocline tanks by using a two-dimensional, two-phase numerical model and they concluded as well that temperature interval had no influence on discharging efficiency.

Taking into account the previous results, general curves can be plotted for dimensionless discharging time, t_{end}^*, thermocline thickness at the end of process, TC_{end}^*, and efficiency, η, all as functions of dimensionless velocity, v^*. These curves are displayed in Fig. 6(a)–(c) respectively and are valid for any thermocline tank, independently on the size, the kind of storage liquid, the presence or not of solid filler and the temperature interval. If we analyse the discharging time, t_{end}^*, (Fig. 6(a)) it obviously decreases as velocity increases, but its real value will depend not only on tank height but also on the thermophysical properties of the storage medium (see (Eq. (7)) and hence on the porosity (see (Eqs. (9), (2), (3)). Thermocline thickness at the end of process (discharge in this case), TC_{end}^*, (Fig. 6(b)) decreases as velocity increases attaining an asymptotic minimum of about 0.26. The contrary happens with the efficiency, η, (Fig. 6(c)) which increases with velocity up to an asymptotic maximum around 87%. This result proves that, comparing with a two-tank storage system a thermocline tank similar in size cannot deliver the same amount of energy already from the theoretical point of view. In this comparison we assume that in both cases there is a certain volume within the tanks that is not available because it is required for the pump's head. The velocity value from which minimum thermocline thickness or maximum efficiency is attained will depend on how accurate the observer is. Actually if we look at Fig. 6(b) and (c) the asymptotic values seem to be reached from $v^* \sim 1900$. However being accurate with the numerical results, 87.3% maximum efficiency and minimum thermocline size of 0.256 are obtained when $v^* \geqslant 2350$. Taking into account this condition together with (Eq. (8)), we obtain the following expression valid for any thermocline tank with liquid as heat transfer fluid:

$$v^* = \frac{(\rho C_p)_{liquid} L v_m}{k_{eff}} \geqslant 2350 \Rightarrow \eta = 87.3\% \qquad (17)$$

This equation provides the minimum dimensionless velocity, v^*, and hence, the minimum velocity of the liquid at tank inlet/outlet, v_m, from which maximum efficiency is achieved. The expression depends on operating conditions through v_m, on tank height, L, and on some properties of the storage medium like effective thermal conductivity and volumetric heat capacity of liquid. It also depends on porosity through the effective thermal conductivity but it is independent on temperature interval and on solid filler heat capacity.

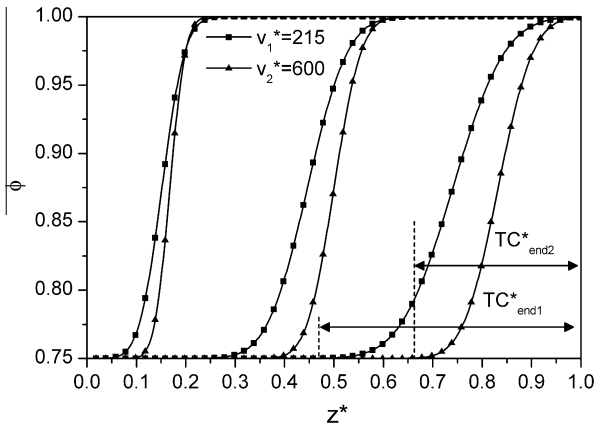

Fig. 4. Dimensionless temperature profiles along tank height at different times for simulations performed with CIEMAT1D1SF model using two dimensionless velocities: $v_1^* = 215$ and $v_2^* = 600$. The thermocline thickness at the end of the process has been indicated for each velocity case.

Table 2
Dimensionless characteristic parameters corresponding to the simulations displayed in Fig. 4.

Results	v^*	
	215	600
t_{end}^*	0.00342	0.00139
TC_{end}^*	0.531	0.337
z_{end}^*	0.736	0.833
η	73.6%	83.3%

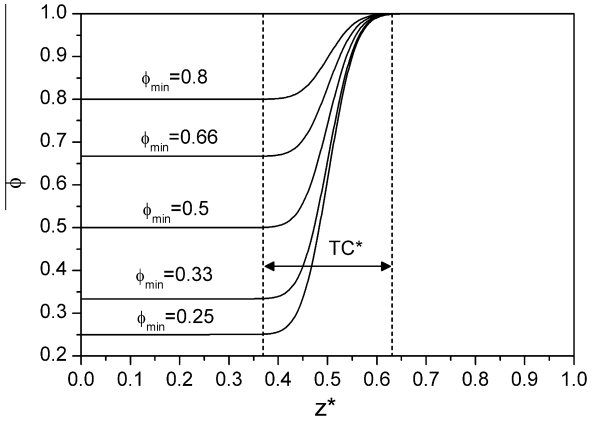

Fig. 5. Dimensionless temperature profiles along tank height when thermocline zone is centered at $z^* = 0.5$ (i.e., in the middle of tank height) for different ϕ_{min} values. Thermocline thickness has been indicated.

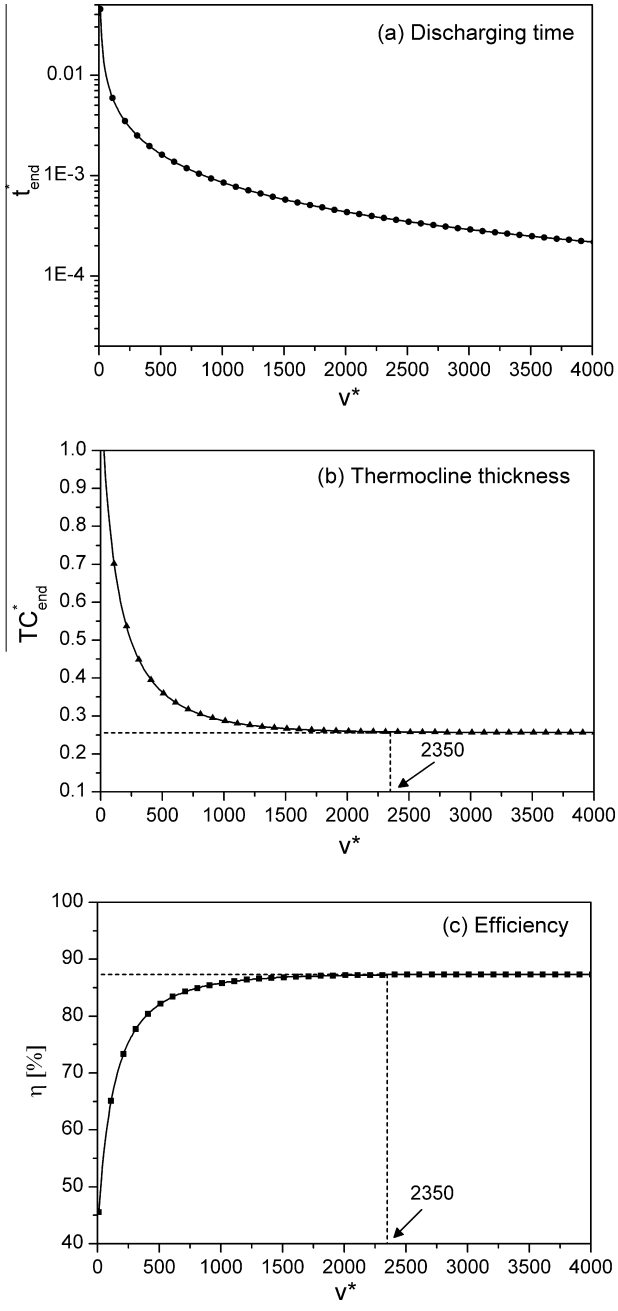

Fig. 6. General curves of discharging time, t^*_{end} (a), thermocline thickness, TC^*_{end} (b) and efficiency η (c) versus dimensionless velocity, v^*. The v^* value from which TC^*_{end} attains the asymptotic minimum and η the asymptotic maximum has been indicated.

We have applied (Eq. (17)) to the particular case of thermocline tanks similar in size and performance to the tanks already existing as storage systems in commercial plants like Andasol I [1] and Gemasolar [2]. The main characteristics and design parameters of these storage tanks are recorded in Table 3. For each kind of plant, two cases have been considered: a tank with only solar salt and hence $\varepsilon = 1$ and a packed-bed tank of porosity $\varepsilon = 0.22$ with quartzite rock and sand (similar to Sandia Prototype) and solar salt. The values of thermophysical properties for the storage materials are those of Table 5. For all cases we obtained v^* values greater than 2350, which means that these thermocline tanks are expected to perform at maximum theoretical efficiency.

Table 3
Main characteristics and design parameters of the two-tank storage systems installed at the commercial plants Andasol I and Gemasolar.

Design parameters	Solar thermal power plant	
	Andasol I [1]	Gemasolar [2]
Power	50 MW_e	20 MW_e
Kind of storage	Two-tank indirect	Two-tank direct
Storage fluid	Solar salt	Solar salt
Storage time, t_{end}	7 h (420 min)	15 h (900 min)
Tank height, L	14 m	10.5 m
Tank diameter, D	36 m	23 m
Temperature interval, $T_{max} - T_{min}$	386–292 °C	565–290 °C
Discharge thermal power	148 MW_{th}	62 MW_{th}
Fluid velocity in discharge, v_{liquid}	2 m/h	0.7 m/h

Xu et al. carried out a parametric study of packed-bed molten salt thermocline tanks similar in performance and size to the Andasol I tanks, by using their own two-phase two-dimensional simulation model [25]. They also obtained that tank efficiency was not influenced either by temperature interval, liquid velocity or porosity. This means that our single-phase one-dimensional model CIEMAT1D1SF is good enough for describing the performance of a packed-bed thermocline tank that is meant to be used as storage system in a solar thermal power plant (i.e. real-size tank).

3.3. Model application: prototypes

The condition to be fulfilled by a thermocline tank performing at maximum efficiency shown by (Eq. (17)) can also be expressed as:

$$v_m L \geqslant \frac{2350 \times k_{eff}}{(\rho C_p)_{liquid}} \tag{18}$$

In this way, for a given storage medium, large values of both tank height and liquid velocity should ensure large dimensionless velocities and hence the highest efficiency. Actually, as we have shown in the previous section, real-size thermocline tanks already display maximum efficiency. However, care must be taken when building small thermocline prototypes because in such case both tank height and liquid velocity are meant to be reduced as a consequence of the down scaling.

In order to analyze the behaviour of a thermocline storage prototype we should remind that liquid velocity at tank inlet/outlet, v_m, is directly related to the thermal power stored/delivered by the tank, P[W], through the equation:

$$\begin{aligned} P &= (C_p)_{liquid}\dot{m}_{liquid}(T_{\max} - T_{\min}) \\ &= 0.25\pi D^2 (\rho C_p)_{liquid} v_m (T_{\max} - T_{\min}) \\ &= 0.25\pi D^2 (\rho C_p)_{eff} v_{TC} (T_{\max} - T_{\min}) \end{aligned} \tag{19}$$

This equation can also be expressed in terms of thermocline zone velocity, v_{TC}, by taking into account (Eq. (11)). Moreover, for calculating thermal power, mass flow is required and hence tank diameter, D, must be introduced as new parameter. Finally, if (Eq. (18)) is substituted in (Eq. (19)) the following expression is obtained:

$$P \geqslant \frac{2350 \times 0.25\pi D^2 \times k_{eff}(T_{\max} - T_{\min})}{L} \tag{20}$$

This expression linking tank dimensions (D and L), storage medium effective conductivity, temperature interval and thermal power, is the design equation for building thermocline storage tanks with maximum theoretical efficiency. Note that the presence of tank diameter, D, comes from the thermal power (Eq. (19)) but not from the simulation model (Eq. (18)), which is one-dimensional and whose results in terms of tank behaviour are indepen-

dent on its diameter. Eq. (20) can be graphically represented by plotting the minimum tank height, L_{min}, required for a certain tank diameter, D, as a function of thermal power, P, for a given temperature interval and a certain storage medium. The corresponding expression is:

$$L_{\min} = \frac{2350 \times 0.25\pi D^2 \times k_{eff}(T_{\max} - T_{\min})}{P} \quad (21)$$

In Fig. 7 the variation of minimum tank height, L_{min}, as a function of thermal power, P, has been represented for thermocline tanks of various diameters, D, containing only solar salt ($\varepsilon = 1$) and working at two different $T_{max} - T_{min}$ intervals: 400–300 °C and 550–300 °C. Similar curves have been plotted in Fig. 8 for a storage medium composed by solar salt and a packed-bed of quartzite rock and sand (similar to Sandia prototype) with $\varepsilon = 0.22$. As stated by (Eq. (21)) for a given thermal power, as D increases L_{min} also increases, which is clearly displayed by the curves recorded in Figs. 7 and 8. However, strong differences are observed in the curves depending on the porosity of the storage medium or which temperature interval is considered. Looking at porosity, we can see that for similar values of both P and D, L_{min} values are lower when $\varepsilon = 1$ (Fig. 7) than when $\varepsilon = 0.22$ (Fig. 8). This happens because in this case $k_{solar\text{-}salt} < k_{solid\text{-}filler}$ (Table 5 of Appendix) and hence $k_{eff}(\varepsilon = 1) < k_{eff}(\varepsilon = 0.22)$. Looking at the temperature interval, it seems clear that the greater the temperature interval, the larger the L_{min} value required for obtaining a thermocline tank with the highest theoretical efficiency.

In order to understand the usefulness of (Eq. (21)) and its applicability in the design process of a thermocline tank, two prototype examples of 100 kW and 1 MW are presented in Table 4. For both of them the storage materials, the porosities and the temperature intervals discussed above have been considered. In each example, tank diameter was increased until the corresponding L_{min} attained a value that was either higher or very close to $L = 16$ m, which has been already established by some authors as the construction vertical limit for metallic tanks [8,26]. Additionally, the thermocline velocity, v_{TC}, corresponding to each diameter and power (Eq. (19)) was calculated and recorded as well in Table 4.

From all prototype possibilities displayed in Table 4 only the highlighted cases can be considered as valid whereas the rest must be disregarded due to different reasons. As said above L_{min} cannot be larger than 16 m (identified by *) if a metallic tank is being constructed. In some cases thermocline velocity, v_{TC} is too low to be used in a tank with such L_{min}, since this would imply charging/discharging times longer than 24 h (identified by #). In other cases the resulting thermocline velocity, v_{TC}, is to our opinion, too high for any tank height associated to the corresponding diameter (identified by †).

In general, low values of L_{min} would enable to build thermocline tanks with a wider range of storage capacities and hence charging/discharging times. Therefore, if we compare prototypes in terms of thermal power, we can see that the 1 MW case leads to more tank size possibilities than the 100 kW case, or, in other words, erecting a 1 MW prototype may be more feasible and appropriate than erecting one of 100 kW. On the other hand, if we compare the

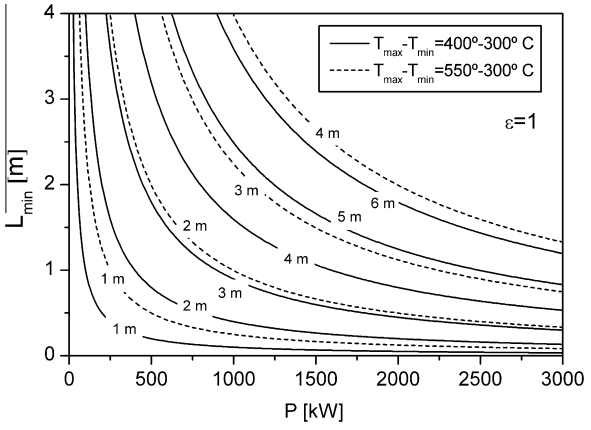

Fig. 7. Variation of minimum tank height, L_{min}, as a function of thermal power, P, for thermocline tanks of various diameters, D, containing only solar salt ($\varepsilon = 1$) and working at two different $T_{max} - T_{min}$ intervals: 400–300 °C and 550–300 °C.

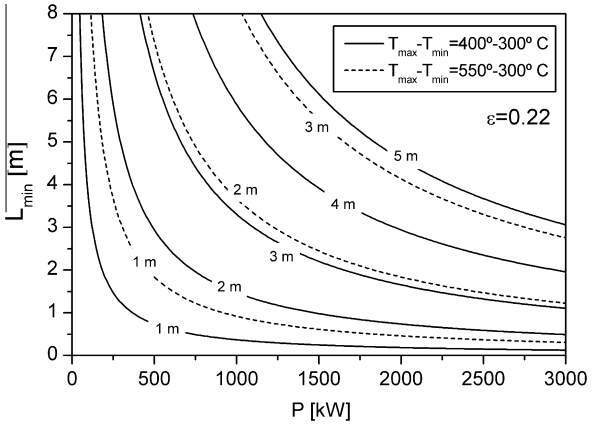

Fig. 8. Variation of minimum tank height, L_{min}, as a function of thermal power, P, for thermocline tanks of various diameters, D, solar salt and a packed-be of quartzite rock and sand ($\varepsilon = 0.22$) and working at two different $T_{max} - T_{min}$ intervals: 400°–300 °C and 550–300 °C.

Table 4
Minimum values of tank height, L_{min}, for two prototype cases: $P = 100$ kW and $P = 1$ MW with different diameters, D, porosities, ε, and temperature intervals $T_{max} - T_{min}$.

$P = 100$ kW						
	$T_{max} - T_{min}$					
	400–300 °C			550–300 °C		
ε	D (m)	L_{min} (m)	v_{TC} (m/h)	D (m)	L_{min} (m)	v_{TC} (m/h)
1	**1**	**1.00**	**1.65**	**1**	**2.49**	**0.66**
	2	**3.98**	**0.41**	2	9.97	0.16#
	3	8.97	0.18#	3	22.43*	0.07#
	4	15.95	0.10#			
0.22	**1**	**2.67**	**1.93**	**1**	**9.18**	**0.77**
	2	14.69	0.48#	2	36.73*	0.19#

$P = 1$ MW						
	$T_{max} - T_{min}$					
	400–300 °C			550–300 °C		
ε	D (m)	L_{min} (m)	v_{TC} (m/h)	D (m)	L_{min} (m)	v_{TC} (m/h)
1	1	0.10	16.46†	**1**	**0.25**	**6.58**
	2	**0.40**	**4.11**	**2**	**1.00**	**1.65**
	3	**0.90**	**1.83**	**3**	**2.24**	**0.73**
	4	**1.59**	**1.03**	**4**	**3.98**	**0.41**
	5	**2.49**	**0.66**	5	6.23	0.26#
	6	**3.59**	**0.46**	6	8.97	0.18#
	7	**4.88**	**0.34**	7	12.21	0.13#
0.22	1	0.37	19.30†	**1**	**0.92**	**7.72**
	2	**1.47**	**4.82**	**2**	**3.68**	**1.93**
	3	**3.31**	**2.1**	**3**	**8.26**	**0.86**
	4	**5.87**	**1.21**	4	14.69	0.48#
	5	**9.18**	**0.77**	5	22.96*	0.31#
	6	13.22	0.54#			
	7	18.99*	0.39#			

* $L_{min} > 16$ m [8,23].
\# Velocity is too low for the L_{min} value.
† Velocity is too high for any $L > L_{min}$.

Table 5
Thermophysical properties of storage liquids and solid filler materials.

Property	Substance				
	Water	Solar salt $60\%NaNO_3 - 40\%KNO_3$	Caloria HT43	Rock + sand (Solar one)	Rock + sand (Sandia prototype)
ρ (kg/m^3)	1000	1857	877	2643	2690
C_p (kJ/kg K)	4.18	1.50	2.70	1.02	0.84
ρC_p (kJ/m^3 K)	4180	2785	2368	2698	2260
k (W/m K)	0.61	0.54	0.09	2.2	2.4

two temperature intervals, we observe that 400–300 °C interval allows more tank size choices than 550–300 °C interval. Finally if we compare prototypes in terms of porosity it is clear that packed-bed tanks with $\varepsilon = 0.22$ are more restricted in size than the tanks with only molten salt and $\varepsilon = 1$.

It must be pointed out here that in the previous discussions we did not consider any restriction for L/D ratio and hence some of the cases recorded in Table 4 might not be feasible from practical point of view. In this way we could take into account the normalized tank dimensions included in the standards Underwriter's Label [27] and API 650 [28] in which L/D ratio for tanks with $D \leqslant 5$ m should be between 1.5 and 4. This means that for example the 100 kW-tank with $\varepsilon = 0.22$, $D = 1$ m and $L_{min} = 9.18$ m should also be excluded from the valid tank sizes as well.

These results demonstrate that from a theoretical point of view some guidelines should be considered when thermocline prototypes with maximum efficiency and hence comparable in behaviour to real-size tanks want to be designed. In this way, the critical parameter determining the design is thermal power because the larger the power the higher the degree of freedom for choosing tank dimensions and hence storage capacity and charging/discharging time.

4. Conclusions

A single-phase one-dimensional model called CIEMAT1D1SF has been developed for simulating thermocline storage tanks with an effective storage medium formed by either a liquid or a liquid and a packed-bed. Although CIEMAT1D1SF can be considered a simplified version of previous models, it has been successfully validated with experimental data taken from the literature and results in terms of thermocline tank behaviour are similar to those obtained with more complex simulation models.

In order to obtain simulation results valid for any kind of thermocline tank with liquid as heat transfer fluid, the thermal equation describing the tank behaviour has been expressed in terms of dimensionless variables and the resulting expression only depends on the parameter called dimensionless velocity, v^*. The influence of v^* in the performance of thermocline tanks has been evaluated in terms of thermocline thickness and discharge tank efficiency.

In this way we observed that thermocline thickness decreased as v^* was increased attaining a minimum value when $v^* \geqslant 2350$. The contrary happened with the tank efficiency, whose value increased with v^* up to a maximum of 87.3% also for $v^* \geqslant 2350$. From these results the design equation for building thermocline storage tanks with maximum theoretical efficiency has been established. This expression links tank dimensions, storage medium effective conductivity, temperature interval and thermal power. Thermocline tanks that might be applied in commercial solar thermal plants like Andasol I and Gemasolar fulfil this condition and hence they are expected to perform at maximum efficiency.

Since the design equation of thermocline tanks with maximum efficiency depends on tank dimensions and thermal power, small thermocline tanks and hence prototypes, are not expected to behave in the same way as large or real-size tanks. In this way guideline plots relating tank dimensions, porosity and thermal power have been presented for different temperature intervals. From these plots the critical design parameter has proven to be thermal power because the larger the power the higher the degree of freedom for choosing tank dimensions and hence storage capacity and charging/discharging time. Therefore, the use of these guideline plots in the design process of thermocline prototypes is highly recommended.

Acknowledgments

The authors would like to acknowledge the E. U. and the 7th Framework Programme for the financial support of this work under the O.P.T.S. project with contract number: 283138.

Appendix A

(Table 5. Thermophysical properties of storage liquids and solid filler materials)

References

[1] S. Relloso, E. Delgado, SolarPaces 2009 Conference, Berlin, Germany, September 2009.
[2] J.I. Burgaleta, S. Arias, D. Ramirez, SolarPACES 2011 Conference, Granada, Spain, September 2011.
[3] Concentrating solar power, Renewable energy technologies: cost analysis series, vol. 1, Power Sector, issue 2/5, IRENA, June 2012.
[4] Kutscher et al., Line-Focus Solar Power Plant Cost Reduction Plan, NREL/TP-5500-48175, Boulder, CO, 2010.
[5] Solar thermocline storage systems: preliminary design study, EPRI, Palo Alto, CA, 2010, 1019581.
[6] C. Libby, L. Derezo, R. Bedilion, J. Pietruszkiewicz, M. Lamar, R. Hollenbach, SolarPACES 2010 Conference, Perpignan, France, September 2010.
[7] T.E.W. Schumann, J. Franklin Inst. 208 (1929) 405–416.
[8] J.E. Pacheco, S.K. Showater, W.J. Kolb, J. Sol.Energy Eng. 124 (2002) 153–159.
[9] G.J. Kolb, V. Hassani, in: Proceedings of ISEC 2006, ASME International Solar Energy Conference, Denver, CO, July 2006.
[10] G.G. Kolb, J. Sol.Energy Eng. 133 (2011) 031023.
[11] Bharathan D, Glatzmaier G. Proceedings of Energy Sustainability Conference, San Francisco, CA, 2009.
[12] Z. Yang, S.V. Garimella, Sol. Energy 84 (2010) 974–985.
[13] C. Xu, Z. Wang, Y. He, X. Li, F. Bai, Appl. Energy 92 (2012) 65–75.
[14] J.T. Van Lew, P. Li, C.L. Chan, W. Karaki, J. Stephens, J. Sol.Energy Eng. 133 (2011). 021003-1-10.
[15] R. Bayón, E. Rojas, E. Rivas, SolarPACES 2012 Conference, Marrakech, Morocco, September 2012.
[16] Y.H. Zurigat, P.E. Liche, A.J. Ghajar, Int. J. Heat Mass Transfer 34 (1991) 115–125.
[17] S.E. Faas, L. Thorne, E. Fuchs, N. Gilbersten, 10 MWe solar thermal central receiver pilot plant: thermal storage subsystem evaluation – Final report, Sandia National Laboratories, SAND86-8212, Albuquerque, CO, June 1986.
[18] W. Zang, K.E. Thompson, A.H. Reed, L. Beenken, Chem. Eng. Sci. 61 (2006) 8060–8074.
[19] M. Mota, J.A. Teixeira, A. Yelshin, Sep. Purif. Technol. 15 (1999) 59–68.
[20] E.E. Gonzo, Chem. Eng. J. 90 (2002) 299–302.
[21] S.V. Patankar, Series in Computational Methods in Mechanics and Thermal Sciences, Taylor & Francis, 1980.

[22] M.Y. Haller, C.A. Cruickshank, W. Streicher, S.J. Harrison, E. Andersen, S. Furbo, Sol. Energy 83 (2009) 1847–1860.
[23] F.J. Oppel, A.J. Ghajar, P.M. Moretti, Appl. Energy 23 (1986) 205–224.
[24] J.D. Cheng, Y. Shin, Sol. Energy 85 (2011) 3010–3016.
[25] C. Xu, Z. Wang, Y. He, X. Li, F. Bai, Renewable Energy 48 (2012) 1–9.
[26] U. Herrmann, B. Kelly, H. Price, Energy 29 (2004) 883–893.
[27] 125.570 Tanks, construction, testing, underwirter's label, Michigan Company Laws, Last version 20/02/2012.
[28] API650: welded steel tanks for oil storage, American Petroleum Institute, 10th Edition 01/11/1998.